What can we infer about the underlying physics from burst distributions observed in an RMHD simulation?

N. W. Watkins[1], S. Oughton[2], M. P. Freeman[1]

[1]British Antarctic Survey (NERC), High Cross, Madingley Road, Cambridge, CB3 0ET, UK

[2]Department of Mathematics, University College London, Gower St, London WC1E 6BT, UK

Abstract

We determine that the sizes of bursts in mean-square current density in a reduced magnetohydrodynamic (RMHD) simulation follow a power-law probability density function (PDF). The PDFs for burst durations and waiting time between bursts are clearly not exponential and could also be power-law. This suffices to distinguish their behaviour from the original Bak et al. sandpile model which had exponential waiting time PDFs. However, it is not sufficient to distinguish between turbulence, some other SOC-like models, and other red noise sources.

1   Introduction

The widespread occurrence of both self-affine time series with "$1/f$" power spectra and spatial fractals in nature led Bak et al. (1987, 1988) (BTW) to propose the hypothesis of self-organised criticality (SOC) (Bak 1997; Jensen 1998; Sornette 2000) as their common origin. Their proposal was based on the demonstration of a "sandpile" cellular automaton (see also the earlier work of Katz (1986)) which appeared to be attracted from arbitrary initial conditions ("self-organisation") to a critical state characterised by fluctuations on all scales in the energy released by the system ("criticality"). Power-law probability density functions (PDFs) for the sizes and durations of energy bursts were the main observed signatures of criticality, and were tested by finite-size scaling of the PDFs with system size (Cardy 1996).

One of the original applications proposed by BTW for their idea was fully developed turbulence, in view of the scaling behaviour of such systems, and the intermittency of their energy dissipation. Furthermore, intermittent turbulence has been an inspiration for later "sandpile"-like cellular automata such as the forest fire model of Bak et al. (1990). The SOC paradigm has since found many applications (Bak 1997; Jensen 1998; Sornette 2000), one of which has been its use by Lu and Hamilton (1991) and subsequent authors to explain the observed power-law distributions for the magnitudes, intensities, and durations of solar flares. SOC has since also been applied to other natural

and artificial plasma confinement systems, notably the Earth's magnetosphere (a recent review is that of Chapman and Watkins (2001)) and tokamaks (e.g. (Chapman et al. 2001)).

In turn, recent studies in the solar flare context, of both shell models (Boffetta et al. 1999) and simulations based more directly on the magnetohydrodynamic (MHD) equations (Georgoulis et al. 1998; Einaudi and Velli 1999) have focused attention on the fundamental questions of the ways in which SOC and turbulence may differ (Boffetta et al. 1999) or, conversely, the extent to which SOC may serve as a model for turbulence (Einaudi and Velli 1999). These more general questions are our main focus in this paper. Also included is some brief discussion of the application of these ideas to solar flares and plasma turbulence in the solar wind, magnetosphere, and elsewhere.

Recent work has shown that magnetically forced 2D MHD turbulence produces power-law PDFs in the size and duration of bursts in spatially averaged Ohmic energy dissipation $\langle \eta J^2 \rangle$ (Georgoulis et al. 1998; Einaudi and Velli 1999) (G98). Recall that such power-law PDFs are a necessary but not sufficient condition for SOC (Jensen 1998). In addition Einaudi and Velli (1999) showed that a cellular automaton with rules chosen to be consistent with the MHD model also produces avalanches (and power-law PDFs).

In contrast, Boffetta et al. (1999) and Giuliani et al. (2000) (B99) attributed the presence of a power-law PDF in the observed waiting time between solar flares to turbulence. Rather than simply being due to the scale-free turbulent cascade itself, B99's suggested mechanism for the production of power law waiting time PDFs was on-off intermittency. They noted that simple prototype models of on-off intermittency and a many-oscillator shell model of turbulence both had waiting time PDFs which were power-law, while the original BTW sandpile algorithm did not, having instead an exponential PDF of waiting times.

Two important criticisms of B99's model and its interpretation have recently been made in the context of solar flares. Einaudi and Velli (1999) pointed out that its attractors were states in which velocity and magnetic field were aligned, whereas they asserted that force free (aligned current and magnetic field) states were probably more appropriate to the corona. Wheatland (2000) showed how a Poisson process varying on a long time scale (e.g. the quasi-periodic solar cycle) could convert an exponential waiting time distribution such as that from the original sandpile model into a power-law one of the type observed.

These results are however less relevant to the more general plasma turbulence case. In physical systems where there is no long-term periodicity to motivate the "periodic-Poisson" assumption of Wheatland (2000) there is no apparent reason to prefer such a mechanism for observed power laws to an intrinsically scale-free one. In addition, the work of Wheatland (2000) seems to have been partly been a response to B99's over-general assertion that all SOC models *must* have exponential waiting time PDFs. This is not true in general (c.f. the discussions in Galtier (2001) and Freeman et al. (2000b); and the models studied by Paczuski et al. (1996)). In consequence, several interesting questions remain open.

One is whether the burst size and duration PDFs found in simulations of 2D MHD turbulence (Georgoulis et al. 1998; Einaudi and Velli 1999) are also observed for either full MHD or reduced MHD (RMHD), in which "slow" k_z dependence is retained, (see below).

The second is whether the power-law waiting time PDFs seen in both the B99 one-dimensional shell model and the Galtier (2001) 1D MHD simulation, are also seen in higher dimensions.

Finally there is the question of whether a minimal set of scale-free "burst" PDFs and power spectra can be identified which suffices to identify SOC (or turbulence) in a physical system. This last question is also highly topical in magnetospheric and laboratory plasmas (cf. Krommes 2000; Freeman et al. 2000b; Kovacs et al. 2001).

In this paper we address these questions by examining time series of various spatial averages of the squared electric current density, $j^2(x, y, z, t)$, drawn from a RMHD simulation. A threshold method, used by previous authors to construct burst-size PDFs, is applied to the time series. Power-laws in size (and arguably also in duration) are found, extending the forced 2D MHD results of Georgoulis et al. (1998) and Einaudi and Velli (1999) to forced RMHD. The PDF of waiting times is also not exponential, confirming that higher-dimensional RMHD is in keeping with the predictions of B99 based on a 1D shell model. Because the fixed threshold method employed detects fractality, which was a predicted feature of SOC but is also generic to red noise, we then consider to what extent the current evidence is unambiguous. We conclude by suggesting a direction for future research.

2 Simulation Data and Analysis

The data analysed here is extracted from a (spectral method) reduced MHD simulation which was used in connection with a model for coronal heating via the coupling of low-frequency Alfvén waves and quasi-2D turbulence (see Oughton et al. (2001) for further details). Using standard (nonlinear) RMHD as a base (Montgomery 1982; Strauss 1976; Zank and Matthaeus 1992), the equations were augmented with terms representing (i) forcing by a single large-scale Alfvénic mode, (ii) reflection of all propagating modes, and (iii) transmission of outward propagating modes. Physically, one may think of reduced MHD as parallel planes of (incompressible) 2D MHD coupled together by a *strong* mean magnetic field ($\mathbf{B}_0$) perpendicular to these planes. *Long* wavelength Alfvén waves propagate along the mean field. Thus, the fluctuating velocity and magnetic fields (respectively $\mathbf{v}$ and $\mathbf{b}$) are functions of all three spatial coordinates, but gradients in the $\mathbf{B}_0$ direction are restricted to be weak. Moreover, $\mathbf{v}$ and $\mathbf{b}$ are strictly perpendicular to $\mathbf{B}_0$.

Here we are primarily interested in various time series characterizing such systems. Specifically, those for the spatially averaged mean-square electric current density $J^2(t) = \langle j^2(x, y, z, t) \rangle / 2$, and the k_z-dependent x- and y-averaged $j^2/2$, denoted as $J^2(t, k_z)$, where k_z is the Fourier wavenumber in the direction parallel to the mean field and angle brackets denote the spatial averaging. Clearly, $J^2(t) = \sum_{k_z} J^2(t, k_z)$.

The particular simulation employed has large-scale Reynolds numbers of 800, a resolution of $256^2 \times 4$, (Alfvénic) forcing of the $\mathbf{k} = (1, 1, 1)$ Fourier mode, and reflection and transmission rates of 1.0 and 0.3, respectively (Oughton et al. 2001). Note that the reflection and transmission parameters are to be interpreted as inverse time scales and not as fractions. The simulation was continued for $500\,T_B$ where T_B is defined as the time taken for a forced Alfven wave to cross the simulation box, which is comparable to the large-scale nonlinear time. After a few tens of T_B, the system settles down into a state which is more or less statistically steady, reminiscent of the similar behaviour of the BTW sandpile (see figure 4.3 of Jensen (1998)). The time series are obtained by calculating the appropriate quantities every 1/10 of a box crossing time, after this steady state has been reached. This sampling interval was chosen in order to have a manageable amount of simulation data. After removing the initial transient, each time series $J^2(k_z, t)$ consists of ≈ 4500 points. The $k_z = 1$ plane is special, since the single forced mode lies in it.

Figure 1a shows the statistically steady portion of the time series of $J^2(t, k_z = 2)$, for which the corresponding PDF and cumulative distribution function (CDF) are shown as Figures 1b and 1c respectively. Inspection of the time series itself (Figure 1a) does not show extreme values to the same extent as e.g. figure 1a of Georgoulis et al. (1998), and so in consequence the PDF we find for it (Figure 1b) is substantially more symmetric. This is illustrated by the dashed line in Figure 1b which shows a Gaussian with the same mean and standard deviation as those of the time series.

To measure the distribution of bursts, a fixed threshold method was employed, as used by Freeman et al. (2000b) (and previous workers, see references therein). The size e of a burst was defined as the integrated area under the curve between a given upward crossing of a fixed threshold and the immediately subsequent downward crossing. The duration T was then the time between upward and downward crossings, while the waiting time (or inter-burst interval, τ) was that between a given downward crossing and the next upward crossing. The resulting PDF for burst size is plotted in Figure 2a, where the solid line indicates the curve corresponding to use of the median value of the time series as the threshold, while the eight dotted lines correspond to those resulting from the 10th, 20th, ..., 40th, 60th through 90th percentiles. PDFs for burst duration and waiting time constructed by the same method are shown in Figures 2b and 2c. The number of bursts bursts thus defined will vary weakly with the threshold chosen, in the case of the median threshold the size distribution $D(e)$ was formed from 198 events. Despite the symmetrical PDF of J^2 shown in Figure 1b, a power-law PDF is obtained for burst sizes in the range 10^{-3} to 2 units (Figure 2a), which remains stable even as the thresholds are varied. Outside this region the points deviate from a power law but their statistical weight is low. The dashed line shown is a power law fit to those points where the number of samples per bin is greater than 4. The PDFs of burst durations and waiting times also resemble power-laws in the range 0.2 to 2, beyond which the number of samples per bin again falls below 5. Similar plots were obtained for all four k_z planes in the simulation, and on averaging over k_z. Figure 2d shows

the PDF for the waiting times plotted on semilog axes, on which an exponential distribution would appear as a straight line, confirming that the waiting times (as defined herein) for this simulation are *not* exponentially distributed.

3   Discussion and Conclusions

We find that the PDF of burst size measured in our simulation is power-law in form, independent of the choice of threshold. The PDFs of duration and waiting time appear to have the same basic form (although the evidence is much less clear cut). Intriguingly, we have observed this property in a time series (Figure 1a) whose PDF (Figure 1b) is not long-tailed but rather symmetric. Power-law burst PDFs are often seen coupled with long-tailed underlying PDFs, and so it is sometimes thought that the scaling range of a signal will be controlled by the mean to peak ratio (governed by σ and μ for Gaussian data, μ for Poisson data, etc.) In fact, however, burst size is also governed by the degree of persistence β in the signal, because it is not just affected by the probability of N points being above a line but is controlled by the probability of N non-independent, successive points all being above the line. Malamud and Turcotte (1999) have noted that β can be varied independently of the PDF of the members of a time series, so that even a time series with a Gaussian distribution of amplitudes but a non-zero β would have a non-negligible probability of several successive values exceeding a threshold. In addition, for such a series, the scaling properties of the distributions of waiting time and inter-burst interval are set entirely by β and would be power laws.

This raises an interesting question, however (see also Freeman et al. (2000b)). Red noise ("$1/f$") time series of the type which SOC systems were originally expected to produce, and whose appearance SOC was proposed to account for, are fractal. The distribution of isosets[1] of such a time series is a power-law (Addison 1997). Hence the burst duration and waiting time PDFs of red noise when found by a threshold method should be power-laws, regardless of whether the noise is produced by turbulence or one of the class of SOC-type models which do produce red noise. The original BTW model can be eliminated as its waiting time series was later shown to be uncorrelated and thus not red noise (Jensen 1998; Boffetta et al. 1999; Freeman et al. 2000b). To determine if a process is SOC in the sense of BTW's original proposal, one needs information about spatial correlations as well as temporal correlations. This is because SOC was proposed as a mechanism linking spatial fractality and temporal persistence ("1/f" noise). This reinforces the point that, rather than simply temporal information (burst durations and waiting times) or avalanche distributions ("burst sizes"), to differentiate between turbulence and SOC it will be necessary to make unambiguous predictions about spatial structure for each phenomenon, requiring at minimum then availability of spatial correlation functions. We note that correlation between bursts e.g. the debated "sympathetic" quality of solar flares (Wheatland et al. 1998) could in principle occur through time or space correlation. This

---

[1] Defined as the set of times at which the time series crosses a fixed level.

line of investigation will be pursued in future papers.

4 Acknowledgements

References

P. S. Addison. *Fractals and Chaos: An Illustrated Course.* Institute of Physics, Bristol, UK, 1997.

P. Bak. *How Nature Works: The Science of Self-Organized Criticality.* Oxford University Press, Oxford, UK, 1997.

P. Bak, C. Tang, and K. Wiesenfeld. Self-organized criticality - an explanation of $1/f$ noise. *Phys. Rev. Lett.*, **59**:381, 1987.

P. Bak, C. Tang, and K. Wiesenfeld. Self-organized criticality. *Phys. Rev. A*, **38**:364, 1988.

P. Bak, K. Chen, and C. Tang. A forest-fire model and some thoughts on turbulence. *Phys. Lett. A*, **147**:297, 1990.

G. Boffetta, V. Carbone, P. Giuliani, P. Veltri, and A. Vulpiani. Power laws in solar flares: Self-organized criticality or turbulence. *Phys. Rev. Lett.*, **83**:4662, 1999.

J. Cardy. *Scaling and Renormalization in Statistical Physics.* Cambridge University Press, Cambridge, UK, 1996.

S. C. Chapman and N. W. Watkins Avalanching and self-organised criticality, a paradigm for geomagnetic activity ? *Space Sci. Rev.*, **95**:293, 2001.

S. C. Chapman, R. O. Dendy and B. Hnat. A sandpile model with tokamak-like enhanced confinement phenomenology. *Phys. Rev. Lett.*, **86**:2814, 2001.

G. Einaudi and M. Velli. The distribution of flares, statistics of magnetohydrodynamic turbulence and coronal heating. *Phys. Plasmas*, **6**:4146, 1999.

M. P. Freeman, N. W. Watkins and D. J. Riley. Evidence for a solar wind origin of the power law burst lifetime distribution of the AE indices. *Geophys. Res. Lett.*, **27**:1087, 2000a.

M. P. Freeman, N. W. Watkins and D. J. Riley. Power law burst and inter-burst interval distributions in the solar wind: turbulence or dissipative SOC? *Phys. Rev. E.*, **62**: 8794, 2000b.

S. Galtier A statistical study of quiet times between flares. *Solar Phys.*, **in press**, 2001.

M. K. Georgoulis, M. Velli, and G. Einaudi. Statistical properties of magnetic activity in the solar corona. *Astrophys. J.*, **497**:957, 1998.

P. Giuliani, V. Carbone, P. Veltri, G. Boffetta, and A. Vulpiani. Waiting time statistics in solar flares. *Physica A*, **280**:75, 2000.

H. J. Jensen. *Self-Organized Criticality: Emergent complex behaviour in physical and biological systems.* Cambridge University Press, Cambridge, UK, 1998.

J. I. Katz A model of propagating brittle failure in heterogenous media. *J. Geophys. Res.*, **91**:10412, 1986.

P. Kovacs, V. Carbone and Z. Vörös. Wavelet-based filtering of intermittent events from geomagnetic time-series. *Planet. Space Sci.*, **in press**, 2001.

J. A. Krommes. Self-organized criticality, long-time correlations, and the standard transport paradigm. *Phys. Plasmas*, **7**:1752, 2000.

E. T. Lu and R. J. Hamilton. Avalanches and the distribution of solar flares. *Astrophys. J.*, **380**:L89, 1991.

B. D. Malamud and D. M. Turcotte. Self-affine time series: I. Generation and analyses. *Advances in Geophysics*, **40**:1, 1999.

D. C. Montgomery. Major disruption, inverse cascades, and the Strauss equations. *Physica Scripta*, **T2/1**:83, 1982.

S. Oughton, W. H. Matthaeus, P. Dmitruk, L. M. Milano, G. P. Zank, and D. J. Mullan. A reduced MHD model of coronal heating driven in open magnetic regions driven by reflected low-frequency Alfvén waves. *Astrophys. J.*, **551**:565, 2001.

M. Paczuski, S. Maslov and P. Bak. Avalanche dynamics in evolution, growth and depinning models. *Phys. Rev. E*, **53**:414, 1996.

D. Sornette. *Critical phenomena in natural sciences. Chaos, fractals, selforganization and disorder: concepts and tools.* Springer-Verlag, Berlin, Germany, 2000.

H. R. Strauss. Nonlinear, three-dimensional magnetohydrodynamics of noncircular tokamaks. *Phys. Fluids*, **19**:134, 1976.

M. Wheatland, P. A. Sturrock and J. M. McTiernan The waiting-time distribution of solar flare hard X-ray bursts *Astrophys. J.*, **509**:448, 1998.

M. Wheatland. The origin of the solar-flare waiting-time distribution. *Astrophys. J.*, **L109-L112**, 2000.

G. P. Zank and W. H. Matthaeus. The equations of reduced magnetohydrodynamics. *J. Plasma Phys.*, **48**:85, 1992.
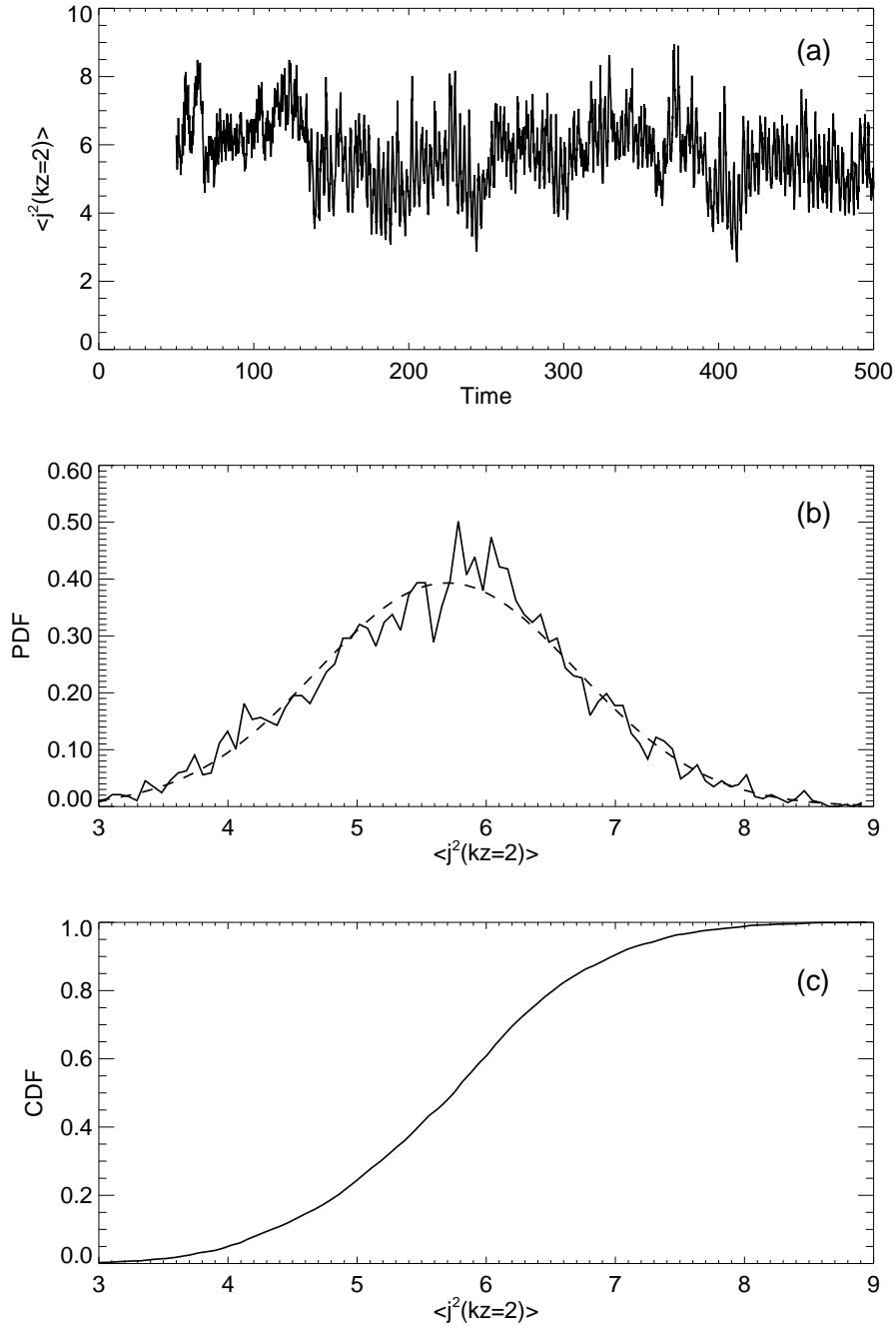
Figure 1: a) Time series of current density for the reduced MHD simulation. b) PDF of current density for the time series in a). Overplotted is a Gaussian distribution with the mean and standard deviation of the time series in Figure 1a. c) CDF of current density for the time series in a).
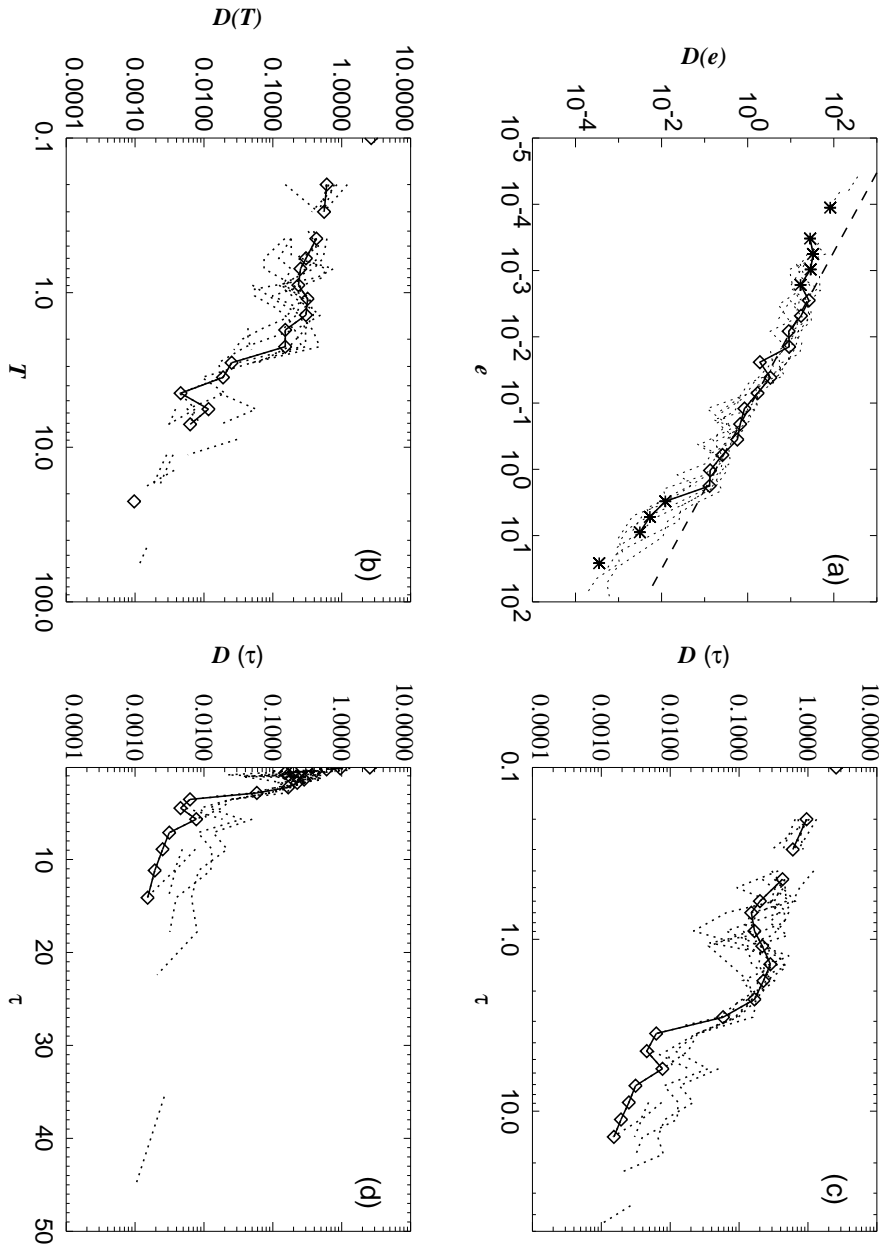
Figure 2: a) Burst size PDF obtained by the threshold method for the time series of Figure 1a). The solid line corresponds to the use of the median of the time series as the threshold while the dotted lines show the 10th, 20th, ... 90th percentiles. The dashed line passes through those points for which a statistically significant number of points is available. b) Burst duration PDF obtained by the method of Figure 2a). c) PDF of waiting times between bursts obtained by the method of Figure 2a). d) The PDF of figure 2c) plotted on a log-linear scale, illustrating that the PDF cannot be fitted well by an exponential.